PCSK9 reduces the protein levels of the LDL receptor in mouse brain during development and after ischemic stroke[S]

Estelle Rousselet,* Jadwiga Marcinkiewicz,* Jasna Kriz,† Ann Zhou,§ Mary E. Hatten, Annik Prat,* and Nabil G. Seidah[1,*]**

Biochemical Neuroendocrinology,* Clinical Research Institute of Montréal (IRCM), Montréal, Québec, Canada; Department of Psychiatry and Neuroscience,† Laval University, Québec City, Québec, Canada; Robert S. Dow Neurobiology Laboratories,§ Portland, OR; and Developmental Neurobiology,** Rockefeller University, New York, NY

Abstract Proprotein convertase subtilisin/kexin type 9 (PCSK9) plays a major role in cholesterol homeostasis through enhanced degradation of the LDL receptor (LDLR) in liver. As novel inhibitors/silencers of PCSK9 are now being tested in clinical trials to treat hypercholesterolemia, it is crucial to define the physiological consequences of the lack of PCSK9 in various organs. LDLR regulation by PCSK9 has not been extensively described during mouse brain development and injury. Herein, we show that PCSK9 and LDLR are co-expressed in mouse brain during development and at adulthood. Although the protein levels of LDLR and apolipoprotein E (apoE) in the adult brain of *Pcsk9*$^{-/-}$ mice are similar to those of wild-type (WT) mice, LDLR levels increased and were accompanied by a reduction of apoE levels during development. This suggests that the upregulation of LDLR protein levels in *Pcsk9*$^{-/-}$ mice enhances apoE degradation. Upon ischemic stroke, PCSK9 was expressed in the dentate gyrus between 24 h and 72 h following brain reperfusion. Although mouse behavior and lesion volume were similar, LDLR protein levels dropped ~2-fold less in the *Pcsk9*$^{-/-}$-lesioned hippocampus, without affecting apoE levels and neurogenesis.[JLR] Thus, PCSK9 downregulates LDLR levels during brain development and following transient ischemic stroke in adult mice.—Rousselet, E., J. Marcinkiewicz, J. Kriz, A. Zhou, M. E. Hatten, A. Prat, and N. G. Seidah. **PCSK9 reduces the protein levels of the LDL receptor in mouse brain during development and after ischemic stroke. *J. Lipid Res.* 2011.** 52: **1383–1391.**

Supplementary key words low density lipoprotein • apolipoprotein E • hypercholesterolemia • brain development • neurogenesis

The proprotein convertase *PCSK9* (1) is the third gene involved in autosomal dominant familial hypercholesterolemia (2). Gain-of-function PCSK9 mutations result in increased levels of plasma low density lipoprotein (LDL) cholesterol (2–4). In contrast, gene disruption (5, 6) and loss-of-function mutations in PCSK9 (3, 7) prevent the degradation of the LDL receptor (LDLR), resulting in a higher clearance of plasma LDL-cholesterol. These seminal findings led to the development of therapies based on PCSK9 inhibition/silencing for the treatment of hypercholesterolemia (8, 9). Although liver LDLR protein levels are reduced in mice injected with PCSK9 (10, 11) or overexpressing PCSK9 in hepatocytes (6), high quantities of PCSK9 can also downregulate LDLR protein levels in extrahepatic tissues such as the lung, adipose, and kidney (12, 13), suggesting that endogenous circulating PCSK9 that originates from hepatocytes (6, 13) may downregulate LDLR protein in others tissues. At adulthood, PCSK9 is highly expressed in liver and is also abundant in the small intestine, as well as in the kidney and brain throughout embryonic development (1). In mouse brain, PCSK9 is transiently expressed in the telencephalon [maximal at embryonic day (E)12.5] and cerebellum [from E17.5 to postnatal day (P)19] (1). At adulthood, it is only significantly expressed in the rostral extension of the olfactory peduncle (RE-OP) (1). In addition, transgenic mice

Abbreviations: BBB, blood-brain barrier; BrdU, bromodeoxyuridine; CNS, central nervous system; CSF, cerebrospinal fluid; E, embryonic day; EGL, external granular layer; FCx, frontal cortex; IGL, internal granular layer; LDLR, LDL receptor; tMCAO, transient middle cerebral artery occlusion; ML, molecular layer; Ob, olfactory bulb; P, postnatal day; PCSK9, proprotein convertase subtilsin kexin 9; PFA, paraformaldehyde; RE-OP, rostral extension of the olfactory peduncle; WT, wild type.

[1]To whom correspondence should be addressed.
e-mail: seidahn@ircm.qc.ca

[S] The online version of this article (available at http://www.jlr.org) contains supplementary data in the form of seven figures.

This work was supported by Canadian Institutes of Health Research (CIHR) Team Grants CTP 82946 and MOP 102741, CIHR Canada Chair 216684, the Strauss Foundation, and a fellowship from the Canadian Heart and Stroke Foundation (E.R.).

Manuscript received 18 January 2011 and in revised form 13 April 2011.

Published, JLR Papers in Press, April 25, 2011
DOI 10.1194/jlr.M014118

expressing enhanced green fluorescent protein (EGFP) under the control of the *Pcsk9* promoter revealed the presence of EGFP in nerve fibers within the olfactory bulb, which is innervated by the RE-OP (National Institutes of Health GENSAT Project) (14).

Although the role of PCSK9 in the brain during mouse development (1) has not been extensively investigated, its overexpression in primary neuronal cultures obtained at E12.5 has been shown to enhance the recruitment of undifferentiated progenitor cells into the neuronal lineage (1). Contrary to PCSK9 knockdown in zebrafish, which results in early death and an extensive disorganization of the central nervous system (CNS) (15), PCSK9 knockout mice are viable (5, 6). Furthermore, we did not observe any gross alterations in adult *Pcsk9*$^{-/-}$ mice in the cerebellum, hippocampus, or cortex (16). In pathological situations, such as induction of neural apoptosis by serum withdrawal, PCSK9 is upregulated (17), and overexpression of PCSK9 in cultured cerebellar granular neurons induces cell death (18), suggesting that PCSK9 may be involved in neural apoptotic processes.

In the present study, we show that PCSK9 and LDLR mRNAs are co-expressed in the same cell layer within the telencephalon at E12.5, the cerebellum at P7, and at adulthood in the RE-OP. As in liver, PCSK9 also enhances LDLR protein degradation during brain development. In contrast, at adulthood within the RE-OP and olfactory bulb, LDLR protein levels are not affected by PCSK9. To investigate the role of PCSK9 following brain injury, we induced a transient ischemic stroke in adult mice (19, 20) and analyzed the expression of PCSK9 in the dentate gyrus from 6 h to 1 week following injury. The data showed that the upregulated PCSK9 reduced LDLR protein levels in the lesioned dentate gyrus without significantly affecting de novo neurogenesis. We also showed that protein levels of apoE were decreased in *Pcsk9*$^{-/-}$ mice during development but not at adulthood or following transient ischemic stroke.

METHODS

Animals

Wild-type (WT) C57BL/6J mice, *Ldlr*$^{-/-}$ C57BL/6J mice (#002207) and *apoE*$^{-/-}$ C57BL/6J mice (#002052) were obtained from The Jackson Laboratory and bred in house. *Pcsk9*$^{-/-}$ and transgenic mice overexpressing V5-tagged PCSK9 in the liver were described previously (6) and were backcrossed for 10 generations to the C57BL/6J genetic background. The mice were housed in the Clinical Research Institute of Montreal (IRCM) animal facility on a 12 h light/dark cycle. All mouse experimentations were approved by the IRCM bioethics committee for animal care.

Tissue collection

E12.5, P7, and adult (three-month-old) mice were euthanized with 2% isoflurane. For Western blot analyses, mouse brains at E12.5, cerebella at P7, RE-OP, and adult olfactory bulbs were dissected and frozen in isopentane at −30°C. For Nissl staining and LDLR immunofluorescence, E12.5 embryonic, P7, and adult brains were frozen at −30°C in isopentane and cut into sagital cryosections (8, 12, and 17 μm thick, respectively). For other immunostainings, P7 mice were transcardially perfused with 0.9% NaCl and then with 4% paraformaldehyde (PFA). Brains were frozen in isopentane at −30°C and cut into coronal sections (12 μm thick).

Mouse ischemic surgery

Transient middle cerebral artery occlusion (tMCAO) was performed on two- to three-month-old WT and *Pcsk9*$^{-/-}$ mice (weight 20-25 g). Under temporary 2% isoflurane anesthesia, unilateral transient focal cerebral ischemia was induced by tMCAO for 1 h, followed by different reperfusion periods (6, 24, 72 h and 1 week) (19, 20). Body temperature was maintained at 37°C using a heating pad and an infrared heating lamp. Under an operating microscope, a 12 mm-long 6-0 silicon-coated monofilament suture (Doccol Corporation) was inserted through the left proximal external carotid artery into the internal carotid artery, and then into the circle of Willis, thus occluding the middle cerebral artery. After 1 h of tMCAO, the filament was withdrawn, blood flow restored to normal, and wounds sutured. The same procedure was performed on sham-operated mice, where the monofilament was not inserted. All animals were allowed ad libitum access to water and food before and after surgery. They were fasted for 3 h before euthanization to standardize LDLR levels in all mice.

For in situ hybridization, brains were removed after 6, 24, 72 h and 1 week of brain reperfusion. To quantify neurogenesis in the dentate gyrus, bromodeoxyuridine (50 mg/kg) (BrdU; Sigma-Aldrich) was injected intraperitoneally 24 h postsurgery, twice a day (with an 8 h interval) for two days. To quantify the lesion size and BrdU-positive cells, mouse brains were removed after 72 h reperfusion, perfused with 50 ml of PBS, frozen in isopentane at −30°C, and cut into coronal cryosections (17 μm thick).

Neurological scores

An expanded six-point scale was used as described previously (21). Behavioral assessments were made at 1, 24, 48, and 72 h after reperfusion. Neurological deficits were scored as follows: 0 = normal; 1 = mild turning behavior with or without inconsistent curling when picked up by the tail, <50% attempts to curl to the contralateral side; 2 = mild consistent curling, >50% attempts to curl to the contralateral side; 3 = strong and immediate consistent curling, mouse holds a curled position for more than 1-2 s, with its nose almost reaching tail; 4 = severe curling progressing into barreling, loss of walking or righting reflex; 5 = comatose or moribund state. At least 8 mice per group were evaluated for each experiment, and scores were averaged for statistical analysis.

In situ hybridization

In situ hybridization on whole-mount embryos, brains, or livers was performed as described previously (1). Briefly, cryosections were fixed in 4% PFA for 1 h, and in situ hybridization was performed using mouse PCSK9 (1), LDLR (15), Furin and PC5/6 (22), mouse SKI-1/S1P (23), and mouse clusterin cRNA probes labeled with ^{35}S-UTP. To generate a mouse clusterin cRNA probe, clusterin cDNA was PCR amplified from an Origene clone (MC203543) using sense 5′- ACCGCCATGAAGATTCTCCTGCTGTGCG-3′ and antisense 5′- CAACCGCGGCTTCCGCACGGCTTTTCC-3′ oligonucleotides. Hybridization was analyzed on X-ray film.

Nissl staining

Brain infarct was assessed by Nissl staining. The relative size of the infarct was measured using image software from the Scion Corporation (Frederick, MD), calculated in arbitrary units (pixels), and expressed as a percentage of the contralateral nonlesioned area (100%) for each section.

Immunohistochemistry

For LDLR visualization, brain cryosections were fixed for 1 h in 4% PFA, incubated with monoclonal mouse LDLR antibody (1:150; R and D Systems), and revealed with Alexa Fluor 488-labeled anti-goat IgGs (1:200). Nuclei were stained with Hoescht 33258 for 5 min (100 μg/ml; Sigma-Aldrich). For staining of cell markers, fixed P7 brain cryosections were incubated with mouse monoclonal anti-calbindin (1:300, Sigma-Aldrich), mouse monoclonal-TAG-1 (1:2, 4D7, kindly provided by Drs. J. Dodd and T. Jessell), and rabbit polyclonal anti-Pax-6 (1:300; Covance). Antigen antibody complexes were revealed by 1 h incubation with corresponding species-specific Alexa Fluor (488 or 555)-tagged antibodies (1:300; Molecular Probes). Nuclei were stained with Hoescht 33258 for 5 min (100 μg/ml; Sigma-Aldrich).

BrdU incorporation into DNA was visualized using a specific antibody (Roche Diagnostics). Brain cryosections were dried and then fixed 5 min in methanol at −20°C, then incubated for 45 min in 2N HCl at 37°C and neutralized in borate buffer for 10 min. Brain slices were incubated overnight with a mouse BrdU antibody (1:100), detected with a biotin-labeled secondary antibody (PerkinElmer), and revealed using the Vectastain kit (Vector Laboratories) and DAB substrate (Zymed Laboratories). BrdU-positive cells in the dentate gyrus were counted on four brain slices regularly spaced for at least five mice for each group. BrdU counts following ischemic stroke were expressed as percentages of counts in the nonlesioned side (fixed at 100%).

Protein analyses

Tissue were homogenized in ice-cold precipitation assay buffer (50 mM Tris-HCl, pH 7.8, 150 mM NaCl, 1% Nonidet P-40, 0.5% sodium deoxycholate, 0.1% SDS) containing a mixture of protease inhibitors (Roche Applied Science). Proteins were separated by 8% SDS-PAGE and visualized using mouse anti-LDLR (1:1,000; R and D Systems), rabbit anti-apoE$^{-/-}$ (1:1,000; Biodesign), goat anti-annexin A2 (1:500; R and D Systems), rabbit anti-β-actin (1:10,000; Sigma-Aldrich), mouse anti-β-tubulin (1:2,000; Sigma-Aldrich), mouse anti-calbindin (1:2,000; Sigma-Aldrich), mouse anti-PCNA (1:500; Vector Laboratories), rabbit anti-cyclin E (1:200; Santa Cruz Biotechnology), mouse anti-NeuN (1:1,000; Chemicon), mouse anti-GFAP (1:5,000; Zymed), rabbit anti-Tuj1 (1:10,000; Covance), mouse anti-synaptophysin (1:1,000; Millipore), rabbit anti-GAP43 (1:1,000), and mouse anti-V5 conjugated to horseradish peroxidase (1:10,000). Bound primary antibody was detected with corresponding species-specific HRP-labeled secondary antibody (Amersham Biosciences) and revealed by enhanced chemiluminescence (Amersham Biosciences). Quantitation was performed on a Storm Imager (Amersham Biosciences) by using the Scion image software (Frederick, MD). Normalization of LDLR levels to β-actin or β-tubulin was obtained.

Statistical analysis

Quantitations are defined as mean ± SEM. The statistical significance of differences between groups was evaluated by Student-Newman-Keuls test or one-way ANOVA (ANOVA test) followed by a Dunnett test. A difference between experimental groups was considered statistically significant at $P < 0.05$.

RESULTS

PCSK9 enhances the degradation of the LDLR in mouse telencephalon at E12.5

We previously demonstrated that during development the expression of PCSK9 is tissue- and time-dependent (1). To define the role of PCSK9 in brain, we first focused on its expression during embryonic development. In situ hybridization revealed that, at E12.5, PCSK9 was expressed only in the liver, small intestine, and telencephalon (**Fig. 1A**), suggesting an early developmental role of PCSK9 in these tissues. In telencephalon, PCSK9 was expressed in the frontal cortex (FCx) (Fig. 1A). The expression of the LDLR was also assessed in adjacent sections and was found to colocalize with all PCSK9 expression sites (arrows in Fig. 1A). Furthermore, immunofluorescence analysis, under nonpermeabilizing conditions that reflect cell surface expression, showed that LDLR protein levels were higher in *Pcsk9*$^{-/-}$ telencephalon than in WT ones (Fig. 1B). LDLR quantitation by Western blot in 10 WT and 13 *Pcsk9*$^{-/-}$ extracts confirmed this observation, and revealed a ∼2.7-fold increase in *Pcsk9*$^{-/-}$ compared with WT telencephalons (Fig. 1C). Nissl staining revealed that the telencephalon organization was not grossly altered in *Pcsk9*$^{-/-}$ mice (Fig. 1D), suggesting that at E12.5 the regulation of LDLR by PCSK9 was not critical for tissue integrity.

PCSK9 enhances the degradation of the LDLR in mouse cerebellum at P7

We previously showed that PCSK9 was expressed in the cerebellum at P7 (1). As assessed by in situ hybridization, PCSK9 mRNA was expressed in the external granular layer (EGL), where it colocalized with the LDLR mRNA (**Fig. 2A**). As in E12.5 telencephalon, cell surface LDLR labeling was higher in *Pcsk9*$^{-/-}$ external granular cells versus WT ones (Fig. 2B). Western blot analysis of five cerebella for each genotype showed that the ∼2.5-fold increase was significant (Fig. 2C). Altogether, these data demonstrate that, at P7, cerebellum PCSK9 locally downregulates the protein levels of the LDLR.

We next determined whether the lack of PCSK9 can alter the development of the cerebellum. Nissl staining revealed a normal cerebellum organization in *Pcsk9*$^{-/-}$ mice, with no gross modification of the EGL, molecular layer (ML), or internal granular cell layer (IGL) (Fig. 2D). This was confirmed by the staining of Purkinje cells with calbindin (supplemental Fig. IA), and of granular cells with anti-Pax-6 and anti-TAG-1, which label the granular cell bodies (24) and axons (25), respectively (supplemental Fig. IB). Although PCSK9 induces ex vivo the recruitment of undifferentiated neural progenitor cells into the neuronal lineage (1), we demonstrated that in vivo the protein levels of markers of cell proliferation (PCNA, Cyclin E), cell differentiation (Calbindin), and synapse (synaptophysin, GAP43) remain unchanged in *Pcsk9*$^{-/-}$ mice (supplemental Fig. II).

At adulthood, PCSK9 does not induce LDLR degradation in the RE-OP or olfactory bulb

In adult brain, PCSK9 mRNA was only expressed in the RE-OP (1), where LDLR was also colocalized (**Fig. 3A**), suggesting that herein PCSK9 could also regulate LDLR protein levels. Because neurons of the RE-OP innervate the olfactory bulb (Ob), we also measured LDLR protein levels in this structure. However, Western blot analyses

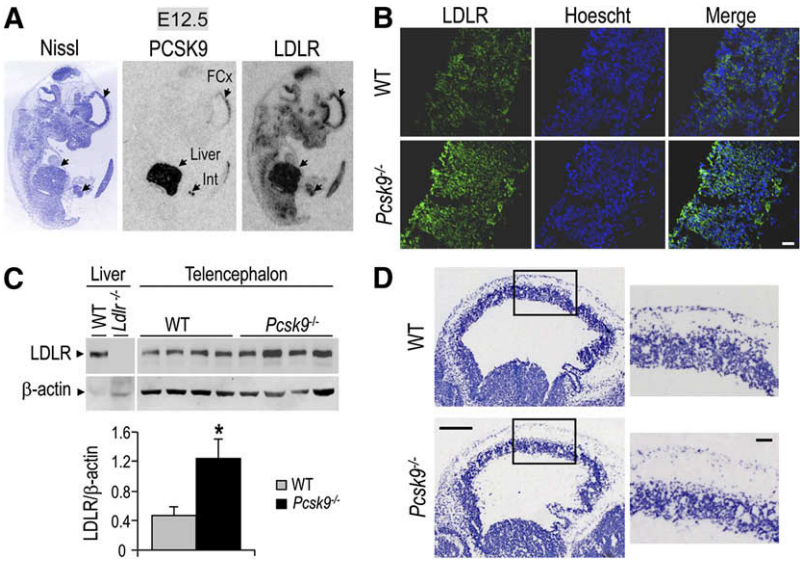

Fig. 1. LDLR regulation by PCSK9 in mouse telencephalon at E12.5. A: PCSK9 and LDLR mRNA distribution pattern in cryosections of sagital mouse embryo at E12.5 by in situ hybridization using PCSK9 and LDLR antisense riboprobes and followed by Nissl staining. FCx, frontal cortex; Int, small intestine. B: Immunofluorescence of LDLR on cryosections of E12.5 WT and *Pcsk9*$^{-/-}$ mice. Nuclei were stained by Hoescht 33258. Bar = 30 μm. C: Representative immunoblots showing LDLR and β-actin protein levels in the telencephalon at E12.5 (100 μg protein load/lane) and in adult liver (30 μg protein load/lane) of WT and *Pcsk9*$^{-/-}$ mice. The specificity of the LDLR antibody is emphasized by the absence of signal in the liver of *Ldlr*$^{-/-}$ mice. Bar diagrams represent the protein levels of LDLR normalized to those of β-actin (n = 10 for WT mice and n = 13 for *Pcsk9*$^{-/-}$ mice). *$P < 0.05$ by Student-Newman-Keuls. All error bars represent SEM. D: Nissl staining showing the cell layer organization in the telencephalon of WT and *Pcsk9*$^{-/-}$ mice. The enlarged squared regions are shown on the right. Bars = 200 μm (left) and 40 μm (right).

demonstrated that the absence of PCSK9 does not affect LDLR protein levels in either the RE-OP or Ob (Fig. 3B). Note that the LDLR is poorly expressed in these structures, as a load of 200 μg protein per lane was required to detect it by Western blot. This may explain why we were not able to sense any immunofluorescence signal in these structures (data not shown). Nissl staining also revealed that the lack of PCSK9 did not affect the organization of the layers in the RE-OP (Fig. 3C) and Ob (Fig. 3D). In addition, Western blot analyses of the cell proliferation (PCNA) and cell differentiation (Tuj-1, NeuN, and GFAP) markers revealed no changes in their protein levels in *Pcsk9*$^{-/-}$ mice (supplemental Fig. III).

PCSK9 is upregulated in the dentate gyrus following an ischemic stroke

To test whether PCSK9 is regulated following a traumatic brain injury, as observed after partial hepatectomy (6), we examined by in situ hybridization the kinetic of its expression in mouse brain following a tMCAO. After 6 h of reperfusion, PCSK9 mRNA was still not detectable in brain areas other than the RE-OP. In contrast, 24 h and 72 h postreperfusion, PCSK9 transcripts were upregulated in the ipsilateral lesioned side of the dentate gyrus, and much less in the contralateral nonlesioned side, and disappeared one week following tMCAO, without significantly affecting the expression of PCSK9 in the RE-OP (**Fig. 4**). This is the first

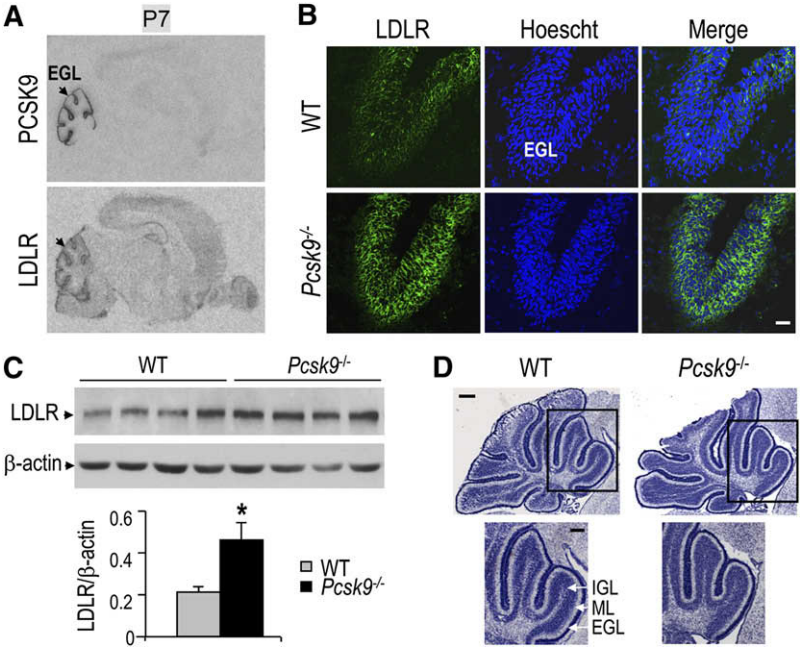

Fig. 2. LDLR regulation by PCSK9 in mouse brain at P7. A: In situ hybridization of sagital mouse brain cryosections at P7 with a PCSK9 and LDLR antisense ^{35}S-labeled cRNA riboprobes. B: Immunofluorescence of LDLR in cerebellum cryosections at P7 from WT and *Pcsk9*$^{-/-}$ mice. Nuclei were stained by Hoescht 33258. Bar = 20 μm. C: Representative immunoblots showing LDLR and β-actin protein levels (100 μg protein load/lane) in the cerebellum of WT and *Pcsk9*$^{-/-}$ mice at P7. Bar diagrams represent the LDLR protein levels normalized to those of β-actin (n = 5 for WT and *Pcsk9*$^{-/-}$ mice). *$P < 0.05$ by Student-Newman-Keuls. All error bars represent the SEM. D: Nissl staining showing the cell layer organization in the cerebellum of WT and *Pcsk9*$^{-/-}$ mice at P7. The enlarged squared regions are shown below. Bars = 250 μm (upper) and 150 μm (lower).

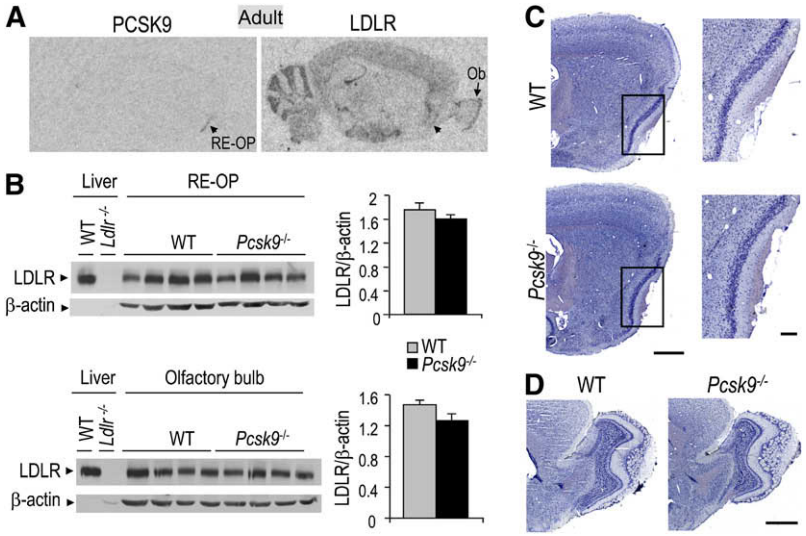

Fig. 3. LDLR regulation by PCSK9 at adulthood. A: In situ hybridization of sagital adult mouse brain cryosections with a PCSK9 and LDLR antisense ^{35}S-labeled cRNA riboprobes. B: Representative immunoblots showing LDLR and β-actin protein levels in the RE-OP and olfactory bulb (200 μg protein load/lane) and in adult liver (30 μg of protein load/lane) of WT and *Pcsk9*$^{-/-}$ mice. The specificity of the LDLR antibody is emphasized by the absence of signal in the liver of *Ldlr*$^{-/-}$ mice. Bar diagrams represent the protein levels of LDLR normalized to those of β-actin in RE-OP and olfactory bulb (n = 9 for WT and *Pcsk9*$^{-/-}$ mice). All error bars represent the SEM. C: Nissl staining showing the structure of the RE-OP in WT and *Pcsk9*$^{-/-}$ mice. The enlarged squared regions are shown on the right. Bars = 400 μm (left) and 100 μm (right). D: Nissl staining revealing the structure of the olfactory bulb in WT and *Pcsk9*$^{-/-}$ mice. Bar = 1 mm.

evidence that PCSK9 mRNA levels are upregulated following a traumatic injury in vivo.

Because tMCAO impacts on behavior in a manner related to the extent of lesion, we measured the lesion volume and mouse behavior following tMCAO (20). The data showed that mouse behavior (scale 2, corresponding to mild consistent curling, with >50% attempts to curl to the contralateral side, see Methods) and lesion volumes of *Pcsk9*$^{-/-}$ mice (~70% compared with the nonlesioned side) did not differ from those of WT mice (**Fig. 5A**, B).

Following tMCAO, PCSK9 was not expressed in the infarct and penumbra areas, suggesting that PCSK9 does not play a significant role in neuronal death. In contrast, it was expressed after ischemic stroke in the dentate gyrus (Fig. 4), a brain area in which neurogenesis takes place (26). Because *Pcsk9*−/− mice exhibited impaired hepatocyte proliferation following partial hepatectomy (6), we tested the impact of PCSK9 on neurogenesis in hippocampus following ischemic stroke. Although cell proliferation, based on BrdU incorporation, tends to increase on the stroke side, in WT and *Pcsk9*−/− mice, our data failed to reveal any significant impact of PCSK9 on the de novo neurogenesis in the dentate gyrus under our tMCAO conditions (Fig. 5C). In addition, hippocampal neurons were healthy as demonstrated by the absence of Fluoro-Jade® B labeling in hippocampus (data not shown). The mRNA expression of clusterin, previously shown to be upregulated and to have a neuroprotective role after permanent middle cerebral artery occlusion (27), was also not modulated in *Pcsk9*$^{-/-}$ dentate gyrus (supplemental Fig. IV).

Interestingly, although hippocampus LDLR protein levels were reduced in WT and *Pcsk9*$^{-/-}$ mice on the lesioned side of the brain after the ischemic stroke, the decrease in LDLR levels was attenuated by 50% in *Pcsk9*$^{-/-}$ mice (**Fig. 6A**). Note that the LDLR protein levels in the nonlesioned side of the hippocampus were similar to those of sham-operated control mice (Fig. 6B). Altogether, our results

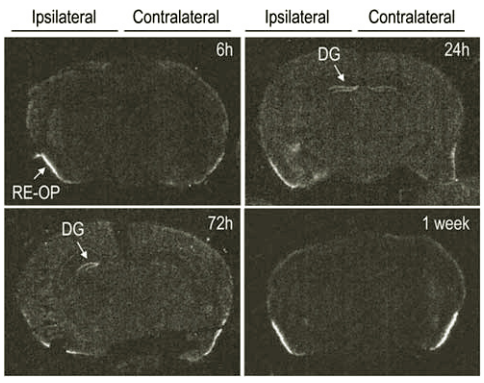

Fig. 4. Time-dependent PCSK9 expression following an ischemic stroke. mRNA distribution pattern using PCSK9 antisense riboprobe, seen as bright labeling under darkfield illumination in mouse coronal cryosections following transient (1 h) tMCAO at different times following brain reperfusion (6, 24, and 72 h and 1 week). DG, hippocampal dentate gyrus.

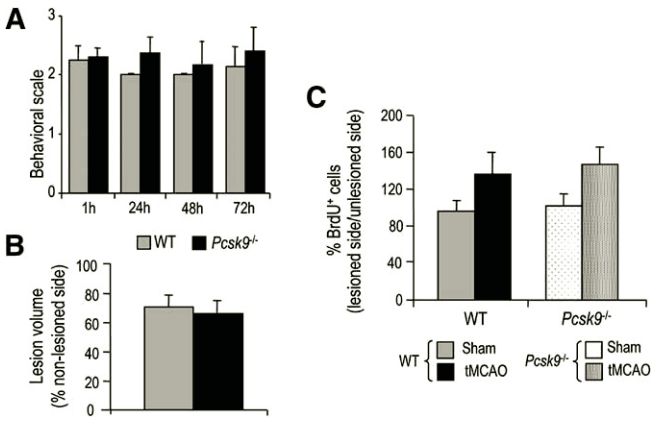

Fig. 5. Impact of ischemic stroke on *Pcsk9*$^{-/-}$ mice. A: Behavior analysis after a tMCAO (1 h) ischemic stroke at different times of brain reperfusion (1, 24, 48, and 72 h) of WT and *Pcsk9*$^{-/-}$ mice. B: Lesion volume at 72 h of brain reperfusion following tMCAO in WT and *Pcsk9*$^{-/-}$ mice. C: BrdU was injected intraperitoneally for two days (twice a day at 8 h intervals) following tMCAO versus in sham-operated mice. WT and *Pcsk9*$^{-/-}$ mice were euthanized at 72 h of brain reperfusion. BrdU positive cells were counted in ipsilateral (lesioned side) and contralateral (nonlesioned side) dentate gyrus. Bar diagrams represent the percent ratio of the number of BrdU positive cells in the ipsilateral side versus the contralateral one (n = 5 for WT and *Pcsk9*$^{-/-}$ mice). All error bars represent the SEM.

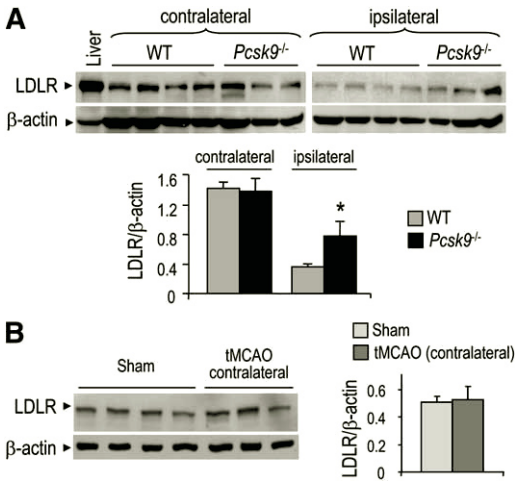

Fig. 6. LDLR regulation by PCSK9 following tMCAO. A: Representative immunoblots showing the protein levels of LDLR and β-actin in the hippocampus of WT and *Pcsk9*$^{-/-}$ mice following tMCAO (1 h) and 24 h of brain reperfusion (200 μg protein load/lane) and in adult liver (30 μg protein load/lane). Ipsilateral and contralateral hippocampi were isolated and analyzed separately. Bar diagrams represent the quantitation of the protein levels of LDLR normalized to those of β-actin (n = 4 for WT and *Pcsk9*$^{-/-}$ mice). *$P < 0.05$ by Dunnett test. All error bars represent the SEM. B: Representative immunoblots showing the protein levels of LDLR and β-actin in the contralateral hippocampus of WT mice following or not tMCAO (1 h) and 24 h of brain reperfusion (200 μg protein load/lane). Bar diagrams represent the quantitation of the protein levels of LDLR normalized to those of β-actin (n = 4 for sham and n = 3 for tMCAO).

suggest that, even though LDLR levels were downregulated following an ischemic stroke, PCSK9 still promotes its degradation.

Downregulation of the protein levels of apoE in Pcsk9$^{-/-}$ mice during development

To determine the role of the regulation of brain LDLR by PCSK9 and because apoE is the main apolipoprotein in brain that can bind LDLR, we quantified the protein levels of apoE during development, at adulthood, and following ischemic stroke. Western blot analyses showed that the ~34 kDa untruncated apoE protein levels were ~25% lower in *Pcsk9*$^{-/-}$ mice in the telencephalon at E12.5 and in the cerebellum at P7 (**Fig. 7A**, B), but not at adulthood in the RE-OP, olfactory bulb, and cerebrospinal fluid (CSF) (Fig. 7C, D). Following ischemic stroke, the ~34 kDa apoE protein levels increased ~1.6-fold in the lesioned dentate gyrus compared with the nonlesioned side (Fig. 7E), consistent with the upregulation of apoE in infarcted cortex and striatum (28). However, no significant difference in the levels of upregulated apoE protein levels between WT and *Pcsk9*$^{-/-}$ mice was observed. Note that the apoE protein levels of sham-operated mice were similar to those of nonlesioned dentate gyrus (data not shown). In addition to the ~34 kDa apoE form, another form running with an apparent molecular weight of ~28 kDa is present at all stages except at P7, as previously reported (29). The protein levels of this apoE form are also not modulated in *Pcsk9*$^{-/-}$ mice. Altogether, these data suggest that the upregulation of LDLR in *Pcsk9*$^{-/-}$ mice enhances apoE degradation only during development, and not at adulthood.

DISCUSSION

The strikingly lower levels of LDL-cholesterol (−40% or −85%) found in individuals carrying loss-of-function mutations on one or both *PCSK9* alleles generated a strong interest from researchers and pharmaceutical industries to develop a PCSK9 inhibitor/silencer for the treatment of dyslipidemias (8, 9). The injection of PCSK9-specific monoclonal antibodies (30) or antisense oligonucleotides in mice (31, 32) and cynomolgus monkeys (33) provided the proof of principle that PCSK9 inhibition/silencing is a promising therapeutic approach for dyslipidemias. It was thus critical to define the clinical phenotypes of the lack of PCSK9 to fully understand its physiological roles in various organs. From this perspective, the impact of the lack of PCSK9 on brain recovery following ischemic stroke was also of interest for future patients who would be treated with a PCSK9 inhibitor/silencer.

We herein demonstrated that, in mouse brain, PCSK9 is co-expressed with the LDLR in the telencephalon at E12.5, cerebellum at P7, and RE-OP at adulthood (Figs. 1–3). The low LDLR protein levels in the RE-OP and olfactory bulb are unchanged in adult *Pcsk9*$^{-/-}$ mice compared with WT mice, suggesting that in adult mice PCSK9 does not promote the degradation of the LDLR in these brain areas (Fig. 3). Our data are consistent with those reported for adult transgenic mice overexpressing PCSK9 in the liver (34), in which no LDLR regulation by ectopic PCSK9 in the adult hippocampus and cortex was observed (1, 6).

However, in the present study we provide the first demonstration that endogenous PCSK9 regulates the levels of LDLR during mouse brain development and following ischemic stroke. Total LDLR protein levels were indeed ⩾2.5-fold higher in the telencephalon at E12.5 and in the cerebellum at P7 of *Pcsk9*$^{-/-}$ embryos or newborns (Figs. 2, 3). Furthermore, they decreased 2-fold less in the *Pcsk9*$^{-/-}$-lesioned dentate gyrus compared with that in WT mice (Fig. 6A). Consistently, cell surface LDLR levels during brain development were increased, suggesting that, as in liver, PCSK9 enhances LDLR internalization and degradation in the analyzed developing or lesioned brain areas. Although annexin A2 has been shown to be an inhibitor of extra-hepatic PCSK9 (35), in *Pcsk9*$^{-/-}$ brain during development and at adulthood, the protein levels of annexin A2 were unchanged compared with those of WT mice (supplemental Fig. V). However, we cannot exclude that, at adulthood, the lack of LDLR regulation by PCSK9 in WT mice is due to a possible modulation of PCSK9 binding to LDLR by annexin A2, especially because LDLR levels are particularly low in the RE-OP.

The absence of V5 immunoreactivity in the CSF of transgenic mice overexpressing V5-tagged PCSK9 in liver (supplemental Fig. VI) demonstrated that circulating PCSK9 does not cross the blood-brain barrier (BBB). This may also explain the absence of brain LDLR regulation by

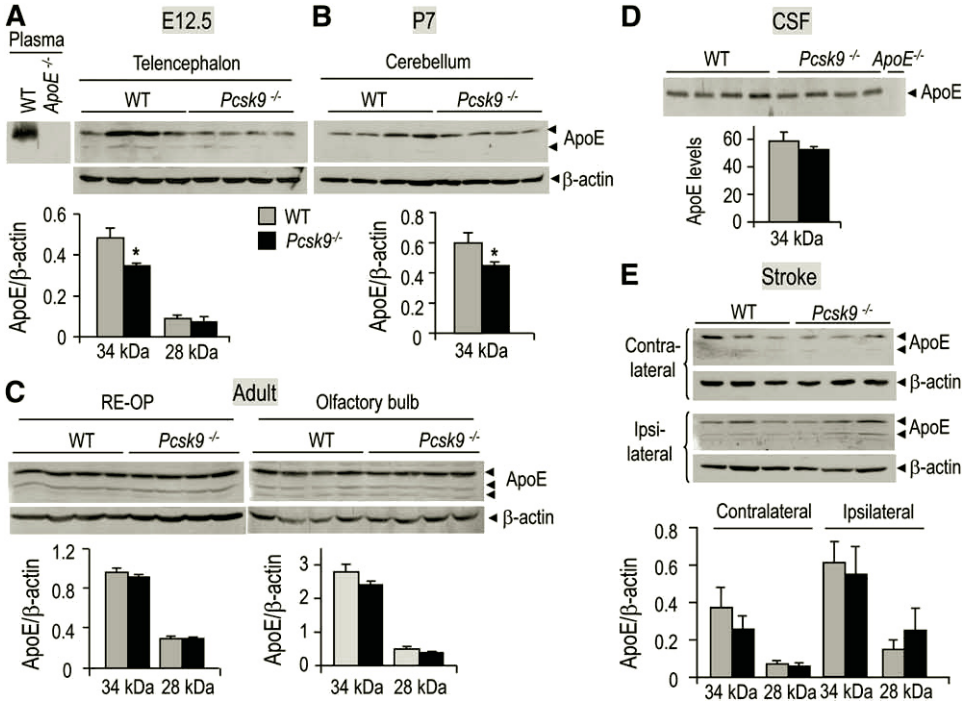

Fig. 7. Regulation of apoE protein levels in *Pcsk9*$^{-/-}$ mouse brain during development, at adulthood, and following tMCAO. Representative immunoblots (100 μg protein load/lane) of WT and *Pcsk9*$^{-/-}$ mice showing the protein levels of apoE and β-actin in the telencephalon at E12.5 (A), in the cerebellum at P7 (B), at adulthood in the REOP and olfactory bulb (C), in adult CSF (D), and in the adult contralateral and ipsilateral hippocampus following tMCAO (E). The specificity of the apoE antibody is emphasized by the absence of signal in the plasma and CSF of *apoE*$^{-/-}$ mice (A, D). Bar diagrams represent the normalized protein levels of apoE to those of β-actin (n = 4). The error bars represent the SEM.

PCSK9 at adulthood. Because the BBB is more permissive at earlier developmental stages and the establishment of its integrity during embryogenesis, or at postnatal stages, has been controversial (36, 37), the potential contribution of circulating PCSK9 in LDLR downregulation at E12.5 and P7 remains to be elucidated. However, the excellent colocalizations of PCSK9 and LDLR expression in the frontal cortex (E12.5) and external granular cell layer (P7) suggest a major contribution of local PCSK9. Furthermore, we showed by in situ hybridization that the expression level of other members of the PC family relevant to cholesterol regulation (Furin, PC5/6, and SKI-1/S1P) (38) do not change upon loss of PCSK9 expression in the liver, where the major expression of PCSK9 occurs (Ref. 1 and supplemental Fig. VII), suggesting that absence of PCSK9 does not influence the mRNA expression of these proprotein convertases (PCs). Consequently, the observed regulation of LDLR levels in *Pcsk9*$^{-/-}$ brain is likely a consequence of the absence of PCSK9.

The physiological and pathological functions of LDLR in the nervous system remain unclear. *Ldlr*$^{-/-}$ mice have normal brain morphology but exhibit impaired learning and memory (39), and the impact of excess LDLR levels on general brain functions has not yet been reported, except in the case of Alzheimer's disease progression (40). However, it has been shown that LDLR has the highest affinity for apoE in brain (41–44). ApoE, a ~34 kDa glycoprotein, is the major apolipoprotein in the brain (45), and it plays an important role in brain cholesterol metabolism. At adulthood, apoE (Fig. 7C, D) and LDLR (Fig. 3B) protein levels are not regulated in the brain of *Pcsk9*$^{-/-}$ mice. Following transient ischemic stroke, in spite of a diminution of LDLR by ~2-fold less in *Pcsk9*$^{-/-}$ mice compared with WT mice, apoE protein levels similarly increased in WT and *Pcsk9*$^{-/-}$ lesioned mice compared with the nonlesioned side (Fig. 7E), suggesting that the ~2-fold higher levels of LDLR in the lesioned hippocampus of *Pcsk9*$^{-/-}$ mice is not sufficient to enhance the general degradation of apoE in brain. However, during brain development, PCSK9 induces a downregulation of the protein levels of the nontruncated apoE form (~25%) (Fig. 7A, B), which may be due to the increase of cell surface LDLR and consequently to an increase in apoE uptake and degradation by lysosomes. This is consistent with the upregulation of apoE protein levels reported in CSF and cortex of *Ldlr*$^{-/-}$ mice (46), and the downregulation by 50-90% of apoE levels in the brain of transgenic mice overexpressing LDLR (40).

The downregulation or degradation of apoE levels by PCSK9, probably through LDLR upregulation, is not enough to induce clear physiological consequences, since during development and following transient ischemic stroke we did not observe any brain morphology alteration or modulation of markers of cell proliferation, cell differentiation, synapses, or clusterin, a neuroprotective protein for ischemic stroke (supplemental Figs. I–IV). Thus, the physiological role of PCSK9 in the brain remains to be defined. Further investigations may be warranted as we cannot exclude from our study that the effect of PCSK9 on

mouse brain is more subtle, since cholesterol is involved in nerve conduction velocity through the formation of myelination and synaptogenesis (47). It also plausible that local hydroxy-cholesterol, rather than circulating cholesterol, is critical for CNS development (48).

Injection of purified PCSK9 or a recombinant adenovirus overexpressing PCSK9 in mice reduced the protein levels of the LDLR in liver, lung, kidney, and small intestine, but not in the adrenal glands (11, 12). In addition, upon overexpression in kidney, the secreted plasma PCSK9 promotes LDLR degradation mostly in the liver and raises plasma LDL (49). Altogether, our data and those in the literature show that not all tissues respond equally to local or circulating PCSK9 and that in adult brain LDLR does not respond to circulating PCSK9. Because the gene ablation of PCSK9 in mice, which completely abolishes PCSK9 expression, does not affect brain organization or brain recovery following ischemic stroke, the silencing of PCSK9, either using monoclonal antibodies (30) or antisense therapies (33) that may partially inhibit PCSK9 expression, should not affect brain PCSK9 levels. However, we cannot exclude that low circulating LDL-cholesterol in treated adult patients with PCSK9-silencing approaches could affect brain LDLR levels via regulation of PCSK9 in the central nervous system (1), likely through the SREBP-2 (50) or HNF-1α pathways (51). Furthermore, rare human subjects exhibiting either PCSK9 loss-of-function mutations [e.g., R46L (3) and R434W (52)] or gain-of-function mutations [e.g., and S127R (2) and D374Y (53)], may during development also exhibit higher or lower levels of LDLR in the brain, respectively, resulting in subtle effects later on in adults.

In conclusion, the present results suggest that PCSK9 inhibition should not interfere with brain development and morphology or with brain recovery/damage after an ischemic stroke. They are consistent with humans carrying heterozygous loss-of-function mutations in PCSK9 who appear healthy and have normal a lifespan (54, 55). Thus, PCSK9 inhibition is likely not to have overt deleterious effects on patients affected by a stroke event and would not be expected to cause major side effects in patients treated with a PCSK9 inhibitor or silencer for hypercholesterolemia.

The authors thank Yuan Cheng Weng for his precious teaching of ischemia procedure and Claudia Toulouse for excellent animal care. Many thanks to all the members of the Seidah laboratory for helpful discussions and to Brigitte Mary for efficacious editorial assistance.

REFERENCES

1. Seidah, N. G., S. Benjannet, L. Wickham, J. Marcinkiewicz, S. B. Jasmin, S. Stifani, A. Basak, A. Prat, and M. Chretien. 2003. The secretory proprotein convertase neural apoptosis-regulated convertase 1 (NARC-1): liver regeneration and neuronal differentiation. *Proc. Natl. Acad. Sci. USA.* **100:** 928–933.
2. Abifadel, M., M. Varret, J. P. Rabes, D. Allard, K. Ouguerram, M. Devillers, C. Cruaud, S. Benjannet, L. Wickham, D. Erlich, et al. 2003. Mutations in PCSK9 cause autosomal dominant hypercholesterolemia. *Nat. Genet.* **34:** 154–156.
3. Kotowski, I. K., A. Pertsemlidis, A. Luke, R. S. Cooper, G. L. Vega, J. C. Cohen, and H. H. Hobbs. 2006. A spectrum of PCSK9 alleles contributes to plasma levels of low-density lipoprotein cholesterol. *Am. J. Hum. Genet.* **78:** 410–422.
4. Allard, D., S. Amsellem, M. Abifadel, M. Trillard, M. Devillers, G. Luc, M. Krempf, Y. Reznik, J. P. Girardet, A. Fredenrich, et al. 2005. Novel mutations of the PCSK9 gene cause variable phenotype of autosomal dominant hypercholesterolemia. *Hum. Mutat.* **26:** 497–506.
5. Rashid, S., D. E. Curtis, R. Garuti, N. N. Anderson, Y. Bashmakov, Y. K. Ho, R. E. Hammer, Y. A. Moon, and J. D. Horton. 2005. Decreased plasma cholesterol and hypersensitivity to statins in mice lacking Pcsk9. *Proc. Natl. Acad. Sci. USA.* **102:** 5374–5379.
6. Zaid, A., A. Roubtsova, R. Essalmani, J. Marcinkiewicz, A. Chamberland, J. Hamelin, M. Tremblay, H. Jacques, W. Jin, J. Davignon, et al. 2008. Proprotein convertase subtilisin/kexin type 9 (PCSK9): hepatocyte-specific low-density lipoprotein receptor degradation and critical role in mouse liver regeneration. *Hepatology.* **48:** 646–654.
7. Cohen, J., A. Pertsemlidis, I. K. Kotowski, R. Graham, C. K. Garcia, and H. H. Hobbs. 2005. Low LDL cholesterol in individuals of African descent resulting from frequent nonsense mutations in PCSK9. *Nat. Genet.* **37:** 161–165.
8. Seidah, N. G. 2009. PCSK9 as a therapeutic target of dyslipidemia. *Expert Opin. Ther. Targets.* **13:** 19–28.
9. Horton, J. D., J. C. Cohen, and H. H. Hobbs. 2009. PCSK9: a convertase that coordinates LDL catabolism. *J. Lipid Res.* **50(Suppl):** S172–S177.
10. Lagace, T. A., D. E. Curtis, R. Garuti, M. C. McNutt, S. W. Park, H. B. Prather, N. N. Anderson, Y. K. Ho, R. E. Hammer, and J. D. Horton. 2006. Secreted PCSK9 decreases the number of LDL receptors in hepatocytes and inlivers of parabiotic mice. *J. Clin. Invest.* **116:** 2995–3005.
11. Grefhorst, A., M. C. McNutt, T. A. Lagace, and J. D. Horton. 2008. Plasma PCSK9 preferentially reduces liver LDL receptors in mice. *J. Lipid Res.* **49:** 1303–1311.
12. Schmidt, R. J., T. P. Beyer, W. R. Bensch, Y. W. Qian, A. Lin, M. Kowala, W. E. Alborn, R. J. Konrad, and G. Cao. 2008. Secreted proprotein convertase subtilisin/kexin type 9 reduces both hepatic and extrahepatic low-density lipoprotein receptors in vivo. *Biochem. Biophys. Res. Commun.* **370:** 634–640.
13. Roubtsova, A., M. N. Munkonda, Z. Awan, J. Marcinkiewicz, A. Chamberland, C. Lazure, K. Cianflone, N. G. Seidah, and A. Prat. 2011. Circulating proprotein convertase subtilisin/kexin 9 (PCSK9) regulates VLDLR protein and triglyceride accumulation in visceral adipose tissue. *Arterioscler. Thromb. Vasc. Biol.* **31:** 785–791.
14. Salero, E., and M. E. Hatten. 2007. Differentiation of ES cells into cerebellar neurons. *Proc. Natl. Acad. Sci. USA.* **104:** 2997–3002.
15. Poirier, S., A. Prat, E. Marcinkiewicz, J. Paquin, B. P. Chitramuthu, D. Baranowski, B. Cadieux, H. P. Bennett, and N. G. Seidah. 2006. Implication of the proprotein convertase NARC-1/PCSK9 in the development of the nervous system. *J. Neurochem.* **98:** 838–850.
16. Seidah, N. G., G. Mayer, A. Zaid, E. Rousselet, N. Nassoury, S. Poirier, R. Essalmani, and A. Prat. 2008. The activation and physiological functions of the proprotein convertases. *Int. J. Biochem. Cell Biol.* **40:** 1111–1125.
17. Chiang, L. W., J. M. Grenier, L. Ettwiller, L. P. Jenkins, D. Ficenec, J. Martin, F. Jin, P. S. DiStefano, and A. Wood. 2001. An orchestrated gene expression component of neuronal programmed cell death revealed by cDNA array analysis. *Proc. Natl. Acad. Sci. USA.* **98:** 2814–2819.
18. Bingham, B., R. Shen, S. Kotnis, C. F. Lo, B. A. Ozenberger, N. Ghosh, J. D. Kennedy, J. S. Jacobsen, J. M. Grenier, P. S. DiStefano, et al. 2006. Proapoptotic effects of NARC 1 (= PCSK9), the gene encoding a novel serine proteinase. *Cytometry A.* **69:** 1123–1131.
19. Belayev, L., R. Busto, W. Zhao, G. Fernandez, and M. D. Ginsberg. 1999. Middle cerebral artery occlusion in the mouse by intraluminal suture coated with poly-L-lysine: neurological and histological validation. *Brain Res.* **833:** 181–190.
20. Beaulieu, J. M., J. Kriz, and J. P. Julien. 2002. Induction of peripherin expression in subsets of brain neurons after lesion injury or cerebral ischemia. *Brain Res.* **946:** 153–161.
21. Jiang, S. X., J. Lertvorachon, S. T. Hou, Y. Konishi, J. Webster, G. Mealing, E. Brunette, J. Tauskela, and E. Preston. 2005. Chlortetracycline and demeclocycline inhibit calpains and protect mouse neurons against glutamate toxicity and cerebral ischemia. *J. Biol. Chem.* **280:** 33811–33818.

22. Seidah, N. G., R. Day, M. Marcinkiewicz, and M. Chretien. 1998. Precursor convertases: an evolutionary ancient, cell-specific, combinatorial mechanism yielding diverse bioactive peptides and proteins. *Ann. N. Y. Acad. Sci.* **839:** 9–24.
23. Seidah, N. G., M. Mbikay, M. Marcinkiewicz, and M. Chretien. 1998. The mammalian precursor convertases: paralogs of the subtilisin/kexin family of calcium-dependent serine proteinases. *In* Proteolytic and Cellular Mechanisms in Prohormone and Neuropeptide Precursor Processing. V. Y. Hook, editor. R.G. Landes Company, Georgetown, TX. 49–76.
24. Gao, W. O., N. Heintz, and M. E. Hatten. 1991. Cerebellar granule cell neurogenesis is regulated by cell-cell interactions in vitro. *Neuron.* **6:** 705–715.
25. Furley, A. J., S. B. Morton, D. Manalo, D. Karagogeos, J. Dodd, and T. M. Jessell. 1990. The axonal glycoprotein TAG-1 is an immunoglobulin superfamily member with neurite outgrowth-promoting activity. *Cell.* **61:** 157–170.
26. Kaplan, M. S., and J. W. Hinds. 1977. Neurogenesis in the adult rat: electron microscopic analysis of light radioautographs. *Science.* **197:** 1092–1094.
27. Imhof, A., Y. Charnay, P. G. Vallet, B. Aronow, E. Kovari, L. E. French, C. Bouras, and P. Giannakopoulos. 2006. Sustained astrocytic clusterin expression improves remodeling after brain ischemia. *Neurobiol. Dis.* **22:** 274–283.
28. Kitagawa, K., M. Matsumoto, K. Kuwabara, T. Ohtsuki, and M. Hori. 2001. Delayed, but marked, expression of apolipoprotein E is involved in tissue clearance after cerebral infarction. *J. Cereb. Blood Flow Metab.* **21:** 1199–1207.
29. Huang, Y., X. Q. Liu, T. Wyss-Coray, W. J. Brecht, D. A. Sanan, and R. W. Mahley. 2001. Apolipoprotein E fragments present in Alzheimer's disease brains induce neurofibrillary tangle-like intracellular inclusions in neurons. *Proc. Natl. Acad. Sci. USA.* **98:** 8838–8843.
30. Chan, J. C., D. E. Piper, Q. Cao, D. Liu, C. King, W. Wang, J. Tang, Q. Liu, J. Higbee, Z. Xia, et al. 2009. A proprotein convertase subtilisin/kexin type 9 neutralizing antibody reduces serum cholesterol in mice and nonhuman primates. *Proc. Natl. Acad. Sci. USA.* **106:** 9820–9825.
31. Graham, M. J., K. M. Lemonidis, C. P. Whipple, A. Subramaniam, B. P. Monia, S. T. Crooke, and R. M. Crooke. 2007. Antisense inhibition of proprotein convertase subtilisin/kexin type 9 reduces serum LDL in hyperlipidemic mice. *J. Lipid Res.* **48:** 763–767.
32. Gupta, N., N. Fisker, M. C. Asselin, M. Lindholm, C. Rosenbohm, H. Orum, J. Elmen, N. G. Seidah, and E. M. Straarup. 2010. A locked nucleic acid antisense oligonucleotide (LNA) silences PCSK9 and enhances LDLR expression in vitro and in vivo. *PLoS ONE.* **5:** e10682.
33. Frank-Kamenetsky, M., A. Grefhorst, N. N. Anderson, T. S. Racie, B. Bramlage, A. Akinc, D. Butler, K. Charisse, R. Dorkin, Y. Fan, et al. 2008. Therapeutic RNAi targeting PCSK9 acutely lowers plasma cholesterol in rodents and LDL cholesterol in nonhuman primates. *Proc. Natl. Acad. Sci. USA.* **105:** 11915–11920.
34. Liu, M., G. Wu, J. Baysarowich, M. Kavana, G. H. Addona, K. K. Bierilo, J. S. Mudgett, G. Pavlovic, A. Sitlani, J. J. Renger, et al. 2010. PCSK9 is not involved in the degradation of LDL receptors and BACE1 in the adult mouse brain. *J. Lipid Res.* **51:** 2611–2618.
35. Mayer, G., S. Poirier, and N. G. Seidah. 2008. Annexin A2 is a C-terminal PCSK9-binding protein that regulates endogenous low density lipoprotein receptor levels. *J. Biol. Chem.* **283:** 31791–31801.
36. Lossinsky, A. S., and R. R. Shivers. 2004. Structural pathways for macromolecular and cellular transport across the blood-brain barrier during inflammatory conditions. Review. *Histol. Histopathol.* **19:** 535–564.
37. Daneman, R., L. Zhou, A. A. Kebede, and B. A. Barres. 2010. Pericytes are required for blood-brain barrier integrity during embryogenesis. *Nature.* **468:** 562–566.
38. Seidah, N. G., and A. Prat. 2007. The proprotein convertases are potential targets in the treatment of dyslipidemia. *J. Mol. Med.* **85:** 685–696.
39. Mulder, M., G. Koopmans, G. Wassink, M. G. Al, M. L. Simard, L. M. Havekes, J. Prickaerts, and A. Blokland. 2007. LDL receptor deficiency results in decreased cell proliferation and presynaptic bouton density in the murine hippocampus. *Neurosci. Res.* **59:** 251–256.
40. Kim, J., J. M. Castellano, H. Jiang, J. M. Basak, M. Parsadanian, V. Pham, S. M. Mason, S. M. Paul, and D. M. Holtzman. 2009. Overexpression of low-density lipoprotein receptor in the brain markedly inhibits amyloid deposition and increases extracellular A beta clearance. *Neuron.* **64:** 632–644.
41. Mahley, R. W. 1988. Apolipoprotein E: cholesterol transport protein with expanding role in cell biology. *Science.* **240:** 622–630.
42. Mahley, R. W., and S. C. Rall, Jr. 2000. Apolipoprotein E: far more than a lipid transport protein. *Annu. Rev. Genomics Hum. Genet.* **1:** 507–537.
43. Innerarity, T. L., and R. W. Mahley. 1978. Enhanced binding by cultured human fibroblasts of apo-E-containing lipoproteins as compared with low density lipoproteins. *Biochemistry.* **17:** 1440–1447.
44. Innerarity, T. L., R. E. Pitas, and R. W. Mahley. 1979. Binding of arginine-rich (E) apoprotein after recombination with phospholipid vesicles to the low density lipoprotein receptors of fibroblasts. *J. Biol. Chem.* **254:** 4186–4190.
45. Elshourbagy, N. A., W. S. Liao, R. W. Mahley, and J. M. Taylor. 1985. Apolipoprotein E mRNA is abundant in the brain and adrenals, as well as in the liver, and is present in other peripheral tissues of rats and marmosets. *Proc. Natl. Acad. Sci. USA.* **82:** 203–207.
46. Fryer, J. D., R. B. Demattos, L. M. McCormick, M. A. O'Dell, M. L. Spinner, K. R. Bales, S. M. Paul, P. M. Sullivan, M. Parsadanian, G. Bu, et al. 2005. The low density lipoprotein receptor regulates the level of central nervous system human and murine apolipoprotein E but does not modify amyloid plaque pathology in PDAPP mice. *J. Biol. Chem.* **280:** 25754–25759.
47. Dietschy, J. M., and S. D. Turley. 2004. Thematic review series: brain lipids. Cholesterol metabolism in the central nervous system during early development and in the mature animal. *J. Lipid Res.* **45:** 1375–1397.
48. Bryleva, E. Y., M. A. Rogers, C. C. Chang, F. Buen, B. T. Harris, E. Rousselet, N. G. Seidah, S. Oddo, F. M. LaFerla, T. A. Spencer, et al. 2010. ACAT1 gene ablation increases 24(S)-hydroxycholesterol content in the brain and ameliorates amyloid pathology in mice with AD. *Proc. Natl. Acad. Sci. USA.* **107:** 3081–3086.
49. Luo, Y., L. Warren, D. Xia, H. Jensen, T. Sand, S. Petras, W. Qin, K. S. Miller, and J. Hawkins. 2009. Function and distribution of circulating human PCSK9 expressed extrahepatically in transgenic mice. *J. Lipid Res.* **50:** 1581–1588.
50. Dubuc, G., A. Chamberland, H. Wassef, J. Davignon, N. G. Seidah, L. Bernier, and A. Prat. 2004. Statins upregulate PCSK9, the gene encoding the proprotein convertase neural apoptosis-regulated convertase-1 implicated in familial hypercholesterolemia. *Arterioscler. Thromb. Vasc. Biol.* **24:** 1454–1459.
51 . Dong, B., M. Wu, H. Li, F. B. Kraemer, K. Adeli, N. G. Seidah, S. W. Park, and J. Liu. 2010. Strong induction of PCSK9 gene expression through HNF1α and SREBP2: mechanism for the resistance to LDL-cholesterol lowering effect of statins in dyslipidemic hamsters. *J. Lipid Res.* **51:** 1486–1495.
52. Davignon, J., G. Dubuc, and N. G. Seidah. 2010. The influence of PCSK9 polymorphisms on serum low-density lipoprotein cholesterol and risk of atherosclerosis. *Curr. Atheroscler. Rep.* **12:** 308–315.
53. Timms, K. M., S. Wagner, M. E. Samuels, K. Forbey, H. Goldfine, S. Jammulapati, M. H. Skolnick, P. N. Hopkins, S. C. Hunt, and D. M. Shattuck. 2004. A mutation in PCSK9 causing autosomal-dominant hypercholesterolemia in a Utah pedigree. *Hum. Genet.* **114:** 349–353.
54. Zhao, Z., Y. Tuakli-Wosornu, T. A. Lagace, L. Kinch, N. V. Grishin, J. D. Horton, J. C. Cohen, and H. H. Hobbs. 2006. Molecular characterization of loss-of-function mutations in PCSK9 and identification of a compound heterozygote. *Am. J. Hum. Genet.* **79:** 514–523.
55. Fasano, T., A. B. Cefalu, E. Di Leo, D. Noto, D. Pollaccia, L. Bocchi, V. Valenti, R. Bonardi, O. Guardamagna, M. Averna, et al. 2007. A novel loss of function mutation of PCSK9 gene in white subjects with low-plasma low-density lipoprotein cholesterol. *Arterioscler. Thromb. Vasc. Biol.* **27:** 677–681.